JOURNAL OF GUIDANCE, CONTROL, AND DYNAMICS
Vol. 21, No. 4, July–August 1998

Decoupling Control Design with Applications to Flight

Antony Snell*
University of California, Davis, Davis, California 95616

Dynamic inversion is presented as a general tool for designing decoupling control laws for multivariable systems, with the difference that instead of using conventional, static, full-state feedback, a dynamic compensator is used. This has the advantages that fewer measurements are required and that the designer has better control over the bandwidth of inner feedback loops. This feature is important because it allows the control law to be made less sensitive to the effects of unmodeled sensor and actuator dynamics, which can be destabilizing. The main focus is on applications to linear systems, although some results may extend to nonlinear systems. The issue of zero dynamics and nonminimum phase is discussed in the linear context. Three examples are presented relating to decoupling of lateral-directional dynamics for highly maneuverable aircraft.

Introduction

THE flight control designer is often faced with the need to design a multivariable control law in which the objective is to decouple the various outputs from each other. This objective may be an end in itself or may yield a starting point for a control design based on single-input/single-output (SISO) techniques. The present paper is a result of the need by the author to reduce the conservatism in the design of a multi-input/multi-output lateral-directional control law using quantitative feedback theory (QFT). QFT is essentially a SISO technique that involves closing one loop at a time,[1] and it was found that cross coupling was the dominant constraint in the design. In Ref. 2 the author found that decoupling the outputs reduced the conservatism significantly. By decoupling the loops before applying QFT, the design is much simpler because the closure of one loop does not affect the performance of the others. The decoupling control law used in Ref. 2 is presented as an example in this paper.

A means for exact decoupling given certain plant characteristics is presented. The basis for the method is dynamic inversion, which has been presented elsewhere as a means of designing nonlinear control laws.[3–7] Unlike conventional dynamic inversion, however, which uses full-state feedback, here a dynamic compensator is used, which is essentially an inverse of the plant. This has the significant advantage that fewer sensors may be required. Furthermore, the decoupling compensator can be designed with low bandwidth so that the effect of unmodeled dynamics can be reduced. It is shown in example 2 that unmodeled dynamics completely destabilized a controller using static feedback only because one of the state feedback loops had an unexpectedly large bandwidth. Although the presentation here is couched in the framework of linear systems, it should also be possible to extend the main ideas to nonlinear plants. For cases where the plant dynamics are stable and the transmission zeros are all located in the left-half plane, the solution is readily obtained using state-space algebra. When the dynamics have right-half plane poles and zeros, the solution is more complex but may be solved by a number of means, which are also discussed.

Dynamic Inversion

Consider the nonlinear system $\boldsymbol{P}$, with state vector $\boldsymbol{x} \in \Re^n$, input vector $\boldsymbol{u} \in \Re^m$, and output vector $\boldsymbol{y} \in \Re^r$:

$$\dot{\boldsymbol{x}} = \boldsymbol{f}(\boldsymbol{x}) + \boldsymbol{g}(\boldsymbol{x})\boldsymbol{u} \tag{1a}$$

$$\boldsymbol{y} = \boldsymbol{h}(\boldsymbol{x}) + \boldsymbol{i}(\boldsymbol{x})\boldsymbol{u} \tag{1b}$$

where $\boldsymbol{f}(\boldsymbol{x})$, $\boldsymbol{g}(\boldsymbol{x})$, $\boldsymbol{h}(\boldsymbol{x})$, and $\boldsymbol{i}(\boldsymbol{x})$ are an n vector, an $n \times m$ matrix, an r vector, and an $r \times m$-matrix of real, continuous functions of $\boldsymbol{x}$ with continuous derivatives, respectively.

Suppose we wish to decouple the r outputs. The procedure for doing this is as follows. If the matrix $\boldsymbol{i}(\boldsymbol{x})$ is right invertible, then the decoupling control law is simply

$$\boldsymbol{u} = \boldsymbol{i}_R^{-1}(\boldsymbol{x})[\boldsymbol{v} - \boldsymbol{h}(\boldsymbol{x})] \tag{2}$$

where $\boldsymbol{v}$ is an r vector of desired values for $\boldsymbol{y}$ and $\boldsymbol{i}_R^{-1}(\boldsymbol{x})$ is the right inverse of $\boldsymbol{i}(\boldsymbol{x})$ such that $\boldsymbol{i}(\boldsymbol{x})\boldsymbol{i}_R^{-1}(\boldsymbol{x}) = \boldsymbol{I}_r$, where $\boldsymbol{I}_r$ denotes the $r \times r$ identity matrix. Substitution of Eq. (2) into Eq. (1) yields the closed-loop dynamics of

$$\dot{\boldsymbol{x}} = \boldsymbol{f}(\boldsymbol{x}) - \boldsymbol{g}(\boldsymbol{x})\boldsymbol{i}_R^{-1}\boldsymbol{h}(\boldsymbol{x}) + \boldsymbol{g}(\boldsymbol{x})\boldsymbol{i}_R^{-1}\boldsymbol{v} \tag{3a}$$

$$\boldsymbol{y} = \boldsymbol{v} \tag{3b}$$

Usually, one or more rows of $\boldsymbol{i}(\boldsymbol{x})$ will be zero. Suppose that the ith row of $\boldsymbol{i}(\boldsymbol{x})$ is zero, then $y_i = h_i(\boldsymbol{x})$. Differentiating with respect to time and using Eq. (1a) yields

$$\dot{y}_i = \sum_{j=1}^{n} \frac{\partial h_i}{\partial x_j}\dot{x}_j = \sum_{j=1}^{n} \frac{\partial h_i}{\partial x_j} f_j(\boldsymbol{x}) + \sum_{k=1}^{m}\sum_{j=1}^{n} \frac{\partial h_i}{\partial x_j} g_{jk}(\boldsymbol{x})u_k \tag{4}$$

which can be expressed in terms of Lie derivatives as

$$\dot{y}_i = L_f h_i(\boldsymbol{x}) + L_g h_i(\boldsymbol{x})\boldsymbol{u} \tag{5}$$

where the operators L_f and L_g are defined by

$$L_f = \sum_{j=1}^{n} f_j(\boldsymbol{x})\frac{\partial}{\partial x_j}, \qquad L_g = \sum_{j=1}^{n} g_j(\boldsymbol{x})\frac{\partial}{\partial x_j}$$

If $L_g h_i(\boldsymbol{x})\boldsymbol{u}$ is zero, Eq. (5) simplifies to

$$\dot{y}_i = L_f h_i(\boldsymbol{x}) \tag{6}$$

and y_i is differentiated again to yield

$$\ddot{y}_i = L_f^{(2)} h_i(\boldsymbol{x}) + L_g L_f h_i(\boldsymbol{x})\boldsymbol{u} \tag{7}$$

If the term in $\boldsymbol{u}$ is still zero, then y_i is differentiated successively until the inputs appear in the derivative expression. The symbol d_i is the smallest number of times that it is necessary to differentiate y_i before $\boldsymbol{u}$ appears. Using the Lie derivative notation gives

$$y_i^{(d_i)} = L_f^{(d_i)} h_i(\boldsymbol{x}) + L_g L_f^{(d_i-1)} h_i(\boldsymbol{x})\boldsymbol{u} \tag{8}$$

Received Nov. 3, 1997; presented as Paper 98-0500 at the AIAA 36th Aerospace Sciences Meeting, Reno, NV, Jan. 12–15, 1998; revision received March 2, 1998; accepted for publication March 6, 1998.

*Assistant Professor, Mechanical and Aeronautical Engineering. Senior Member AIAA.

For each of the outputs y_i, a d_i is found. Then Eq. (8) can be rewritten in matrix form

$$\begin{bmatrix} y_1^{(d_1)} \\ \vdots \\ y_i^{(d_i)} \\ \vdots \\ y_r^{(d_r)} \end{bmatrix} = \boldsymbol{F}(\boldsymbol{x}) + \boldsymbol{E}(\boldsymbol{x})\boldsymbol{u} \tag{9}$$

where $\boldsymbol{F}(\boldsymbol{x})$ and $\boldsymbol{E}(\boldsymbol{x})$ are an r vector function and an $r \times m$ matrix function with rows defined by the following:

$$F_i(\boldsymbol{x}) = \begin{cases} h_i(\boldsymbol{x}) & \text{for} \quad d_i = 0 \\ L_f^{(d_i)} h_i(\boldsymbol{x}) & \text{for} \quad d_i \geq 1 \end{cases} \tag{10a}$$

and

$$E_i(\boldsymbol{x}) = \begin{cases} \boldsymbol{i}_i(\boldsymbol{x}) & \text{for} \quad d_i = 0 \\ L_g h_i(\boldsymbol{x}) & \text{for} \quad d_i = 1 \\ L_g L_f^{(d_i - 1)} h_i(\boldsymbol{x}) & \text{for} \quad d_i \geq 2 \end{cases} \tag{10b}$$

Here the shorthand notation of

$$\boldsymbol{y}^{(d)} = L_f^{(d)} \boldsymbol{h}(\boldsymbol{x}) + L_g L_f^{(d-1)} \boldsymbol{h}(\boldsymbol{x})\boldsymbol{u} \tag{11}$$

will substitute for the definitions in Eq. (10). If the matrix $\boldsymbol{E}(\boldsymbol{x}) \equiv L_g L_f^{(d-1)} \boldsymbol{h}(\boldsymbol{x})$ is right invertible, then it is again possible to construct a decoupling control law

$$\boldsymbol{u} = \boldsymbol{E}_R^{-1}(\boldsymbol{x})\left[\boldsymbol{v} - L_f^{(d)} \boldsymbol{h}(\boldsymbol{x})\right] \tag{12}$$

Substituting Eq. (12) for $\boldsymbol{u}$ into Eq. (11) yields the simple decoupled relationships between the r vector of pseudoinputs $\boldsymbol{v}$ and the outputs $\boldsymbol{y}$

$$y_i^{(d_i)} = v_i \tag{13}$$

Problems arise when the matrix $\boldsymbol{E}(\boldsymbol{x})$ is not right invertible. This occurs in a number of situations.

1) It occurs when there are fewer controls than outputs, $m < r$. In this case, the problem must be reformulated either with more controls or with fewer demands on decoupling of outputs.

2) There may not be enough independent controls. For example, lateral thrust vectoring and rudder have a similar effect on the aircraft dynamics, and so they cannot be used effectively to control two variables independently. Again it is necessary to reformulate the problem as in case 1.

3) Sometimes a solution may be found by appending the control deflections $\boldsymbol{u}$ to the states $\boldsymbol{x}$ and treating the derivatives $\dot{\boldsymbol{u}}$ as the new inputs as discussed in Slotine and Li.[8]

4) There are many occasions when $\boldsymbol{E}(\boldsymbol{x})$ is nearly singular and taking the inverse leads to very large control demands. Again this is a warning that the problem is poorly formulated, and either additional independent inputs should be supplied or demands on the decoupling of outputs should be eased.

Another problem exists with the so-called zero dynamics.[8] These are the internal dynamics of the decoupled system that result from closing the state feedback loops. They can be examined by substituting Eq. (12) for $\boldsymbol{u}$ into Eq. (1). The resulting n-state system contains both the controlled dynamics set according to Eq. (13) and the internal dynamics, which are unobservable in the outputs $\boldsymbol{y} = \boldsymbol{h}(\boldsymbol{x})$. The internal dynamics of a nonlinear system are dependent on the particular choice of the pseudoinput $\boldsymbol{v}$. The zero dynamics are usually defined to be the internal dynamics that result when $\boldsymbol{v}$ is set identically to zero.[8]

Dynamic Inversion for Linear Systems

The approach discussed in the preceding section can be readily applied to linear systems. It should be apparent, however, that this approach requires full-state feedback to compute all of the $\boldsymbol{f}$, $\boldsymbol{g}$, and $\boldsymbol{h}$ functions required in the control law, Eq. (12). Consider the linear time-invariant system $\boldsymbol{P}(s)$ with state vector $\boldsymbol{x} \in \Re^n$, input vector $\boldsymbol{u} \in \Re^m$, and output vector $\boldsymbol{y} \in \Re^r$:

$$\dot{\boldsymbol{x}} = \boldsymbol{A}\boldsymbol{x} + \boldsymbol{B}\boldsymbol{u} \tag{14a}$$

$$\boldsymbol{y} = \boldsymbol{C}\boldsymbol{x} + \boldsymbol{D}\boldsymbol{u} \tag{14b}$$

The state feedback approach just used for the nonlinear dynamic inversion will be reduced to the linear system case. For the linear system, $\boldsymbol{f}(\boldsymbol{x}) = \boldsymbol{A}\boldsymbol{x}$, $\boldsymbol{g}(\boldsymbol{x}) = \boldsymbol{B}$, $\boldsymbol{h}(\boldsymbol{x}) = \boldsymbol{C}\boldsymbol{x}$, and $\boldsymbol{i}(\boldsymbol{x}) = \boldsymbol{D}$. By analogy with Eqs. (9–12) the following are obtained:

$$\boldsymbol{y}^{(d)} = \begin{bmatrix} y^{d_1} \\ \vdots \\ y^{d_i} \\ \vdots \\ y^{d_r} \end{bmatrix} = \boldsymbol{F}\boldsymbol{x} + \boldsymbol{E}\boldsymbol{u} \tag{15}$$

where the rows of matrices $\boldsymbol{F}$ and $\boldsymbol{E}$ are given by analogy to Eq. (10) and noting that $L_f^{d_i} h_i(\boldsymbol{x}) = \boldsymbol{C}_i \boldsymbol{A}^{d_i}$, $L_g h_i(\boldsymbol{x}) = \boldsymbol{C}_i \boldsymbol{B}$, and $L_g L_f^{(d_i - 1)} h_i(\boldsymbol{x}) = \boldsymbol{C}_i \boldsymbol{A}^{(d_i - 1)} \boldsymbol{B}$, which gives

$$[\boldsymbol{E}] = \begin{bmatrix} \boldsymbol{E}_1 \\ \cdots \\ \boldsymbol{E}_i \\ \cdots \\ \boldsymbol{E}_r \end{bmatrix} \tag{16a}$$

where

$$\boldsymbol{E}_i = \begin{cases} \boldsymbol{D}_i & \text{for} \quad d_i = 0 \\ \boldsymbol{C}_i \boldsymbol{A}^{d_i - 1} \boldsymbol{B} & \text{for} \quad d_i \geq 1 \end{cases}$$

and

$$[\boldsymbol{F}] = \begin{bmatrix} \boldsymbol{F}_1 \\ \cdots \\ \boldsymbol{F}_i \\ \cdots \\ \boldsymbol{F}_r \end{bmatrix} \tag{16b}$$

where

$$\boldsymbol{F}_i = \begin{cases} \boldsymbol{C}_i & \text{for} \quad d_i = 0 \\ \boldsymbol{C}_i \boldsymbol{A}^{d_i} & \text{for} \quad d_i \geq 1 \end{cases}$$

By analogy to Eq. (12), a full-state feedback, dynamic inversion is derived as

$$\boldsymbol{u} = \boldsymbol{E}_R^{-1}(\boldsymbol{v} - \boldsymbol{F}\boldsymbol{x}) \tag{17}$$

Substituting Eq. (17) into Eqs. (14a) and (15) yields the closed-loop dynamics

$$\dot{\boldsymbol{x}} = \left(\boldsymbol{A} - \boldsymbol{B}\boldsymbol{E}_R^{-1}\boldsymbol{F}\right)\boldsymbol{x} + \boldsymbol{B}\boldsymbol{E}_R^{-1}\boldsymbol{v} \tag{18a}$$

$$\boldsymbol{y}^{(d)} = \boldsymbol{v} \tag{18b}$$

It is shown in the Appendix that the poles of the zero dynamics are located at the transmission zeros of the open-loop system described by Eqs. (14a) and (14b). This is seen readily in the case that $\boldsymbol{D}$ is nonzero and has full row rank so that it has a right inverse $\boldsymbol{D}_R^{-1}$. Then Eq. (17) becomes

$$\boldsymbol{u} = \boldsymbol{D}_R^{-1}(\boldsymbol{v} - \boldsymbol{C}\boldsymbol{x}) \tag{19}$$

This yields the closed-loop dynamics

$$\dot{\boldsymbol{x}} = \left(\boldsymbol{A} - \boldsymbol{B}\boldsymbol{D}_R^{-1}\boldsymbol{C}\right)\boldsymbol{x} + \boldsymbol{B}\boldsymbol{D}_R^{-1}\boldsymbol{v} \tag{20a}$$

$$\boldsymbol{y} = \boldsymbol{v} \tag{20b}$$

The outputs are decoupled, $y_i = v_i$. The eigenvalues of $(\boldsymbol{A} - \boldsymbol{B}\boldsymbol{D}_R^{-1}\boldsymbol{C})$ in Eq. (20a) are the poles of the zero dynamics of the decoupled system. These are also the transmission zeros of the original system with inputs $\boldsymbol{u}$ and outputs $\boldsymbol{y}$. The transmission zeros are the

values of s for which the system matrix, shown in Eq. (21), loses rank. This reduces to finding a scalar ζ_p and two nonzero vectors z_P and w_P such that

$$\begin{bmatrix} (\zeta_p I - A) & -B \\ C & D \end{bmatrix} \begin{bmatrix} z_P \\ w_P \end{bmatrix} = \begin{bmatrix} 0 \\ 0 \end{bmatrix} \tag{21}$$

A solution to this is given by solving the second row for w_P in terms of z_P and then substituting into the first row to give

$$w_P = -D_R^{-1} C z_P \tag{22a}$$

$$\left(\zeta_p I - A + B D_R^{-1} C\right) z_P = 0 \tag{22b}$$

Thus, the transmission zeros of $P(s)$, ζ_p, are simply the eigenvalues of the matrix $(A - BD_R^{-1}C) = A_G$ and, therefore, are the zero dynamics of the closed-loop system. The right zero direction vector z_P is a right eigenvector of A_G.

Dynamic Inversion for Linear Systems Using Dynamic Compensation

Full-state feedback has a number of drawbacks: 1) A lot of sensors are needed. 2) It is unclear how many states should really be included or whether a reduced-order model would suffice. 3) The effect of unmodeled dynamics is unclear. 4) Robustness analysis of the closed loop is made more difficult because of the multiple-loop closures.

As a consequence of points 2–4, it will be seen that neglecting the actuator dynamics in the design of one of the examples using static state feedback actually led to instability in the presence of the neglected dynamics. This was because the location of a transmission zero at $s = -60$ led to the bandwidth of one of the state feedback loops being unexpectedly high.

For these reasons, an alternative using a dynamic compensator is presented. This compensator $G(s)$ is constructed such that $P(s)G(s) = \text{diag}(1/s^{d_i})$. When the system is diagonalized in this way, it is easier to devise a simple diagonal controller to give satisfactory closed-loop dynamics. In the case that $P(s)$ has an invertible D matrix, then $d_i = 0$, for $i = 1, \ldots, r$, and $P(s)G(s) = I_r$. Otherwise, $G(s)$ may be found by defining $P'(s)$:

$$P'(s) = \text{diag}(s^{d_i}) \cdot P(s) \tag{23}$$

$P'(s)$ has the state-space realization $[A, B, F, E]$, where E and F are defined by Eq. (16). If E has a right inverse E_R^{-1}, then the decoupling system $G(s)$ giving $P(s)G(s) = \text{diag}(1/s^{d_i})$ can be found. Starting with Eqs. (17) and (18a), instead of using actual state measurements x a dynamic system is used to construct an estimated set of states x_G to replace x:

$$\dot{x}_G = A_G x_G + B_G v \tag{24a}$$

$$u = C_G x_G + D_G v \tag{24b}$$

where

$$A_G = \left(A - B E_R^{-1} F\right) \tag{25a}$$

$$B_G = B E_R^{-1} \tag{25b}$$

$$C_G = -E_R^{-1} F \tag{25c}$$

$$D_G = E_R^{-1} \tag{25d}$$

With the dynamics defined in this way, u produced by Eq. (24b) is identical to that produced by the full-state feedback, provided that the initial conditions on x and x_G are identical. Thus, the derivatives of the outputs $y^{(d)}$ are identically equal to v, the input to $G(s)$, and so a decoupling control law has been obtained. If the initial conditions on x and x_G are not identical, then it is necessary to examine the error dynamics. From the definition of $P'(s)$ and A_G, B_G, C_G, and D_G we have

$$y^{(d)} = Fx + Eu = F(x - x_G) + v \tag{26a}$$

$$\dot{x} = Ax + Bu = Ax - B E_R^{-1} F x_G + B E_R^{-1} v \tag{26b}$$

$$\dot{x}_G = \left(A - B E_R^{-1} F\right) x_G + B E_R^{-1} v \tag{26c}$$

where $y^{(d)}$ contains the error term $F(x - x_G)$. The dynamics of the error are found by subtracting Eq. (26c) from Eq. (26b):

$$(\dot{x} - \dot{x}_G) = A(x - x_G) \tag{27}$$

The error decays according to the eigenvalues of A, the open-loop poles of $P(s)$. Note, too, that the error is not controllable via the pseudoinput v and that although the error is observable in $y^{(d)}$, the states x, and x_G are not. All of this is a result of the pole-zero cancellations between $P(s)$ and $G(s)$.

The poles of $G(s)$ are the eigenvalues of A_G, which are the transmission zeros of $P(s)$ (Appendix). Conversely, the transmission zeros of $G(s)$ are given by

$$\begin{bmatrix} (\zeta_G I - A_G) & -B_G \\ C_G & D_G \end{bmatrix} \begin{bmatrix} z_G \\ w_G \end{bmatrix} = \begin{bmatrix} 0 \\ 0 \end{bmatrix} \tag{28}$$

Substituting the definitions of Eq. (25) into (28) gives the transmission zeros of $G(s)$ as

$$\begin{bmatrix} \left(\zeta_G I - A + B E_R^{-1} F\right) & -B E_R^{-1} \\ -E_R^{-1} F & E_R^{-1} \end{bmatrix} \begin{bmatrix} z_G \\ w_G \end{bmatrix} = \begin{bmatrix} 0 \\ 0 \end{bmatrix} \tag{29}$$

The solution is found in a way similar to before:

$$w_G = F z_G \tag{30a}$$

$$\left(\zeta_G I - A + B E_R^{-1} F - B E_R^{-1} F\right) z_G \equiv (\zeta_G I - A) z_G = 0 \tag{30b}$$

The transmission zeros of $G(s)$ are the eigenvalues of A, the poles of $P(s)$. The right zero directions are right eigenvectors of A.

From the foregoing discussion it is clear that $G(s)$ is the right inverse of $P'(s)$. This presents problems for systems with right-half plane poles and/or right-half plane zeros. These cannot be inverted exactly using the realization of Eq. (25) alone because the resulting system will not be internally stable. The inversion can be modified, however, to handle $P(s)$ with right-half plane poles as discussed shortly.

$P'(s)$ is the transfer function from u to $y^{(d)}$, and it has the state-space realization $[A, B, F, E]$. Because the Laplace transform of $y_i^{(d_i)}(t)$ is $s^{d_i} y_i(s)$, the transfer function between u and $y_i^{(d_i)}(t)$ has d_i zeros at $s = 0$, which ensures that $P'(s)$ has relative degree zero and, thus, has a proper, realizable inverse given by $G(s)$. The transfer function matrix relating v to y is the diagonal system

$$P(s)G(s) = \text{diag}(1/s^{d_i}) \tag{31}$$

in which the controlled variable $y^{(d)}$ is identically equal to the input v.

A variation on this design is to realize that the additional zeros added to make $P'(s)$ invertible do not actually have to be located at $s = 0$. They could be located anywhere at the discretion of the designer. For example, $P'(s)$ may be redefined as follows:

$$P'(s) = \text{diag}[q_i(s)] \cdot P(s) \tag{32}$$

where each $q_i(s)$ is a polynomial of degree exactly d_i. Then it is easy to construct $G(s)$ so that $P'(s)G(s) = I_r$. With this choice of $G(s)$ we have

$$P(s)G(s) = \text{diag}[1/q_i(s)] \tag{33}$$

The zeros in each $q_i(s)$ appear as poles of the product $P(s)G(s)$. All that remains is to find a realization for $P'(s)$. This requires us to find new E and F matrices instead of those defined by Eq. (16). Suppose

$$q_i(s) = a_{i0} s^{d_i} + a_{i1} s^{(d_i - 1)} + \cdots + a_{ij} s^{(d_i - j)} + \cdots + a_{id_i} \tag{34}$$

Then define z by

$$z_i = a_{i0} y_i^{d_i} + a_{i1} y_i^{(d_i - 1)} + \cdots + a_{ij} y_i^{(d_i - j)} + \cdots + a_{id_i} y_i \tag{35}$$

$$z_i = a_{i0} C_i A^{(d_i - 1)} B u + a_{i0} C_i A^{d_i} x + a_{i1} C_i A^{(d_i - 1)} x + \cdots + a_{ij} C_i A^{(d_i - j)} x + \cdots + a_{id_i} C_i x \tag{36}$$

The ith row of the new E and F matrices is now given by

$$E_i = a_{i0}C_iA^{(d_i-1)}B \tag{37a}$$

$$F_i = \sum_{j=0}^{d_i} a_{ij}C_iA^{(d_i-j)} \tag{37b}$$

Plants with Right-Half Plane or Poorly Damped Poles

Plants with unstable poles or lightly damped complex poles can be handled by a number of methods. If the procedure of Eqs. (25) is used as it stands, the resulting product, $P(s)G(s)$, contains unacceptable, pole-zero cancellations in the right-half plane. One way of avoiding this is to stabilize the poles using an inner loop before computing $G(s)$. Such an arrangement is used in example 1, where feedback of yaw rate to rudder via the washout $G_r(s)$ was included to provide better damping of the Dutch-roll mode. $G(s)$ was then computed for the stabilized plant. The transfer function between v and y for the combination of the plant and inverter is not changed by closing the inner loops, but the internal modes are better behaved. With the inner loops closed, all the pole-zero cancellations between the plant and the inverter are located in the left-half plane. In the design of example 1, it was found that if the inner loop was not closed the lightly damped, Dutch-roll poles produce lightly damped zeros in the inverse system. When model uncertainty is introduced, these poles and zeros do not cancel each other and the undesirable, lightly damped modes reappear. Furthermore, even if cancellations are exact, Eq. (27) shows that poorly damped eigenvalues of A will lead to slowly decaying errors between x_G and x, which degrades the decoupling performance. The effect of input disturbances is also poor.

Another approach is to treat the inverse system as an observer of the plant and to feedback any additional measurements that might be available, such as the yaw rate. This causes the inverse system states x_G to track the plant states x more accurately, which gives increased robustness to model uncertainty. The observer-based decoupler is similar to the inverse system described by Eq. (25) with one additional term in the expression for $\dot{x}_G$

$$\dot{x}_G = \left(A - BE_R^{-1}F\right)x_G + BE_R^{-1}v + H_{\text{obs}}(x - x_G) \tag{38a}$$

$$u = E_R^{-1}(v - Fx_G) \tag{38b}$$

The term $H_{\text{obs}}(x - x_G)$ in Eq. (38a) is selected to cause x_G to converge exponentially to x. Notice that in the nominal case, where $x_G = x$, the addition of this term does not alter the input–output properties of $P(s)G(s)$. In example 2, H_{obs} was selected to be a diagonal matrix, but this is not a requirement. Following the same procedure as Eqs. (26) and (27), the signal $y^{(d)}$ is examined. In the more general decoupling of Eqs. (35–37), the signal z would be studied instead of $y^{(d)}$:

$$y^{(d)} = Fx + Eu = F(x - x_G) + v \tag{39a}$$

$$\dot{x} = Ax + Bu = Ax - BE_R^{-1}Fx_G + BE_R^{-1}v \tag{39b}$$

$$\dot{x}_G = \left(A - BE_R^{-1}F\right)x_G + BE_R^{-1}v + H_{\text{obs}}(x - x_G) \tag{39c}$$

Once again $y^{(d)}$ contains the error term $F(x - x_G)$, but now the error dynamics are found by subtracting Eq. (39c) from Eq. (39b):

$$(\dot{x} - \dot{x}_G) = (A - H_{\text{obs}})(x - x_G) \tag{40}$$

The addition of the error term in Eq. (38a) does not alter the transfer function between v and y at all, but it does allow the designer to tailor the error dynamics, which are now governed by the eigenvalues of the matrix $(A - H_{\text{obs}})$. The poles of all internal and external modes of $P(s)G(s)$ are given by the roots of

$$\begin{aligned} 0 &= \det\begin{bmatrix} (sI - A) & -BE_R^{-1}F \\ H_{\text{obs}} & \left(sI - \left(A - BE_R^{-1}F - H_{\text{obs}}\right)\right) \end{bmatrix} \\ &= \det\begin{bmatrix} (sI - A + H_{\text{obs}}) & (sI - (A - H_{\text{obs}})) \\ H_{\text{obs}} & \left(sI - \left(A - BE_R^{-1}F - H_{\text{obs}}\right)\right) \end{bmatrix} \\ &= \det\begin{bmatrix} (sI - (A - H_{\text{obs}})) & 0 \\ H_{\text{obs}} & \left(sI - \left(A - BE_R^{-1}F\right)\right) \end{bmatrix} \end{aligned} \tag{41}$$

A subset of the poles is located at the eigenvalues of $(A - H_{\text{obs}})$, whereas the remaining poles are located at the eigenvalues of $(A - BE_R^{-1}F)$, which are the transmission zeros of $P'(s)$, and cannot be altered using H_{obs}. Because the error feedback terms do not affect the nominal transfer function between v and y, they may be selected to be of any reasonable magnitudes to stabilize the poles of $P(s)$ without resorting to inappropriately large magnitudes.

Example 1: Lateral-Directional Decoupling of HARV

In Ref. 2 it was desired to find a control law to decouple sideslip β and roll rate p for the F-18 high-angle-of-attack research vehicle (HARV) aircraft. The open-loop aircraft has a moderate level of coupling between these two outputs. The basic configuration is shown in Fig. 1. The model has five control effectors, which are ganged into two groups with u_1 to control yaw motion and u_2 to control roll:

$$\begin{bmatrix} \delta_{\text{diff.tail}} \\ \delta_{\text{aileron}} \\ \delta_{\text{rudder}} \\ \delta_{\text{diff.TVC}} \\ \delta_{\text{lat.TVC}} \end{bmatrix} = Ku = \begin{bmatrix} 0 & 0.6 \\ 0 & 1.0 \\ 1.0 & 0 \\ 0 & 0.6 \\ 0.6 & 0 \end{bmatrix} \begin{bmatrix} u_1 \\ u_2 \end{bmatrix} \tag{42}$$

There were 15 flight conditions considered, ranging from Mach = 0.3–0.9 and altitude h from 10,000–30,000 ft. A nominal model, Mach = 0.6 and h = 20,000 ft, was selected to provide a single decoupling law for use at all flight conditions. The matrices A_{ac}, B_{ac}, and C_{ac}, given in Table 1, define the rigid-body, lateral-directional dynamics at the nominal condition. The control actuators were modeled by the second-order devices given in Table 2. The Dutch-roll damping was improved by feeding back yaw rate to u_1 via a washout filter $G_r(s)$, whose transfer function is given in Table 3.

The state-space model used in the design of $G(s)$ has A, B, and C matrices consisting of the rigid-body model of the aircraft (3 states),

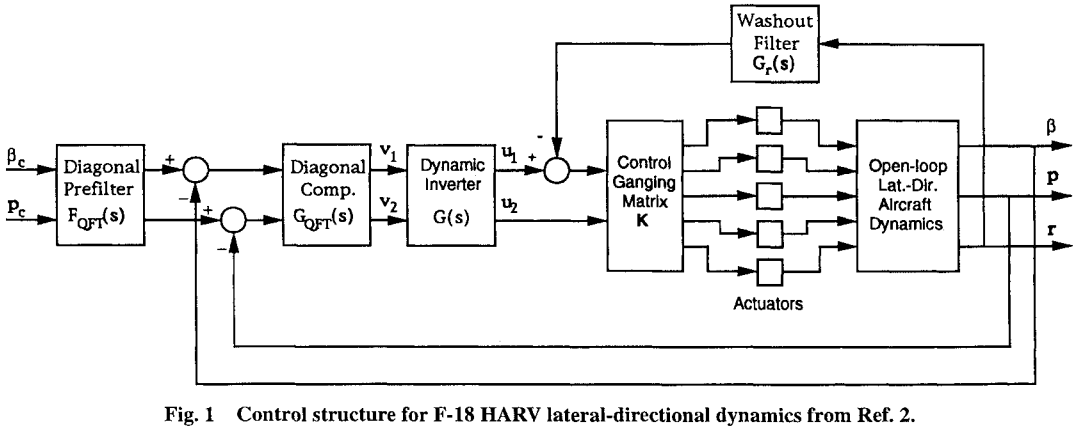

Fig. 1 Control structure for F-18 HARV lateral-directional dynamics from Ref. 2.

Table 1 Rigid-body dynamics F-18 HARV model

$$A_{ac} = \begin{bmatrix} -0.166 & 0.0629 & -0.9971 \\ -12.97 & -1.761 & 0.5083 \\ 3.191 & -0.01417 & -0.1529 \end{bmatrix}$$

$$B_{ac} = \begin{bmatrix} -0.0142 & -0.00686 & 0.01851 & 0 & 0.005817 \\ 14.38 & 16.76 & 1.316 & 0.7007 & 0.0402 \\ 0.3389 & -0.385 & -1.051 & -0.00475 & -0.5511 \end{bmatrix}$$

$$C_{ac} = \begin{bmatrix} 1 & 0 & 0 \\ 0 & 1 & 0 \end{bmatrix}$$

Table 2 Actuator dynamics F-18 HARV model[a]

Actuator	Differential Tail	Aileron	Rudder	Roll TVC[b]	Yaw TVC
ω_n	30	75	72	20	20
ζ	0.707	0.59	0.69	0.60	0.60

[a]All of form $G_{act}(s) = \omega_n^2/(s^2 + 2\zeta\omega_n s + \omega_n^2)$. [b]Thrust vector control.

Table 3 Outer-loop controllers F-18 HARV model

$$G_{QFT}(s) = \begin{bmatrix} \dfrac{1666.6(s+0.3)^2(s+20)}{s(s+1)(s+100)^2} & 0 \\ 0 & \dfrac{22200(s+0.5)(s+20)(s+30)}{s(s+100)^3} \end{bmatrix}$$

$$F_{QFT}(s) = \begin{bmatrix} \dfrac{0.12(s+100)}{(s+3)(s+4)^2} & 0 \\ 0 & \dfrac{1000}{(s+20)(s+50)} \end{bmatrix}$$

Yaw rate washout filter: $G_r(s) = -3s/(s+1)$

to which are appended the washout filter dynamics (1 state) and the five second-order actuators (10 states) with the static control ganging of Eq. (42) giving a total of 14 states. Because of the second-order actuator dynamics, the transfer functions between inputs u_1 and u_2 and outputs β and p, all have relative degree three. Thus, it is necessary to determine the third derivatives of the outputs before the inputs to the actuators appear. Because $1/s^3$ is inherently hard to stabilize, the following transfer function for $\boldsymbol{P}(s)\boldsymbol{G}(s)$ was selected:

$$\boldsymbol{P}(s)\boldsymbol{G}(s) = \text{diag}\left(\frac{900}{s(s+30)^2}\right) \tag{43}$$

This has an ideal integrator form up to about 10 rad/s and then rolls off more quickly at frequencies above 30 rad/s. It makes sense to roll off like this because the bandwidths of the actuators are in the range 20–75 rad/s. The outer-loop compensators $\boldsymbol{G}_{QFT}(s)$ and prefilter $\boldsymbol{F}_{QFT}(s)$ are given in Table 3. The outer-loop crossovers are at $\omega_\beta = 3$ rad/s and $\omega_p = 10$ rad/s. Following the procedure of Eqs. (32–34), define $\boldsymbol{P}'(s)$

$$\boldsymbol{P}'(s) = \text{diag}(q_i(s)) \cdot \boldsymbol{P}(s) \tag{44}$$

where $q_1(s) = q_2(s) = s(s+30)^2/900$. Then $\boldsymbol{E}$ and $\boldsymbol{F}$ are given by

$$\boldsymbol{F} = (1/900)(900\boldsymbol{CA} + 60\boldsymbol{CA}^2 + \boldsymbol{CA}^3) \tag{45a}$$

$$\boldsymbol{E} = (1/900)(\boldsymbol{CA}^2\boldsymbol{B}) \tag{45b}$$

where $\boldsymbol{E}$ defined this way is right invertible, and so it is possible to compute a state-space realization of $\boldsymbol{G}(s)$, the right inverse of $\boldsymbol{P}'(s)$, by substituting Eqs. (45a) and (45b) into Eq. (25):

$$\boldsymbol{A}_G = \boldsymbol{A} - \boldsymbol{B}(\boldsymbol{CA}^2\boldsymbol{B})^{-1}(900\boldsymbol{CA} + 60\boldsymbol{CA}^2 + \boldsymbol{CA}^3) \tag{46a}$$

$$\boldsymbol{B}_G = 900\boldsymbol{B}(\boldsymbol{CA}^2\boldsymbol{B})^{-1} \tag{46b}$$

$$\boldsymbol{C}_G = -(\boldsymbol{CA}^2\boldsymbol{B})^{-1}(900\boldsymbol{CA} + 60\boldsymbol{CA}^2 + \boldsymbol{CA}^3) \tag{46c}$$

$$\boldsymbol{D}_G = 900(\boldsymbol{CA}^2\boldsymbol{B})^{-1} \tag{46d}$$

Because $\boldsymbol{P}'(s)\boldsymbol{G}(s) = \boldsymbol{I}$, the relationship between $\boldsymbol{v}$ and β and p is given by

$$\begin{bmatrix} \beta(s) \\ p(s) \end{bmatrix} = \begin{bmatrix} \dfrac{900}{s(s+30)^2} & 0 \\ 0 & \dfrac{900}{s(s+30)^2} \end{bmatrix} \begin{bmatrix} v_1(s) \\ v_2(s) \end{bmatrix} \tag{47}$$

As reported in Ref. 2, this control design yields very good decoupling with the nominal aircraft model, which provides a good starting point for the QFT design of the main compensator $\boldsymbol{G}_{QFT}(s)$ and prefilter $\boldsymbol{F}_{QFT}(s)$, shown in Fig. 1. The primary disadvantage is the large number of states (14 in all), which makes scheduling with flight condition impractical. The inability to schedule means that the decoupling degrades at flight conditions far from the chosen nominal condition.

Figure 2 shows the Bode magnitude plots v_1 to β for the whole set of 15 flight conditions, whereas Fig. 3 shows the equivalent plots but with the decoupling carried out without the yaw rate feedback. The transmission from v_1 to β is most affected by the poorly damped Dutch-roll mode, and the off-nominal responses in Fig. 3 show significant degradation in the critical 1–10 rad/s flight control region. This degradation occurs because the lightly damped zeros in $\boldsymbol{G}(s)$ no longer cancel the poles in $\boldsymbol{P}(s)$.

Example 2: Improved Decoupling Design for F-18 HARV

A second approach to decoupling control for the F-18 HARV is based on using the partial state feedback described by Eqs. (38–41). The block diagram is shown in Fig. 4. Notice that the separate yaw rate loop has been eliminated. Instead all available measurements are fed directly into $\boldsymbol{G}(s)$. The decoupling controller is further simplified, compared to example 1, by neglecting the actuator dynamics in the design of $\boldsymbol{G}(s)$, which reduces the inverse system from 14 states down to only 3 states. $\boldsymbol{G}(s)$ is now based on only an approximation of the full-order 13 state plant. However, such a simplification allows $\boldsymbol{G}(s)$ to be scheduled more easily with flight condition because there are far fewer parameters to vary. For comparison purposes, a decoupling controller was also designed using direct static feedback of p, r, and β in a conventional dynamic inversion.

The new design commenced by setting $\boldsymbol{A} = \boldsymbol{A}_{ac}$, $\boldsymbol{B} = \boldsymbol{B}_{ac}\boldsymbol{K}$, and $\boldsymbol{C} = \boldsymbol{C}_{ac}$ corresponding to the three-state rigid-body model only and the control ganging matrix $\boldsymbol{K}$ from Eq. (42):

$$\dot{\boldsymbol{x}} = \begin{bmatrix} \dot{\beta} \\ \dot{p} \\ \dot{r} \end{bmatrix} = \boldsymbol{Ax} + \boldsymbol{Bu} \tag{48a}$$

$$\boldsymbol{y} = \begin{bmatrix} \beta \\ p \end{bmatrix} = \boldsymbol{Cx} \tag{48b}$$

Because the second-order, actuator dynamics have been neglected, the dynamics between $\boldsymbol{u}$ and p and β are both of relative degree one. The desired, decoupled dynamics were selected to be the first-order relations

$$\begin{bmatrix} \beta \\ p \end{bmatrix} = \begin{bmatrix} 1/(s+1) & 0 \\ 0 & 1/(s+1) \end{bmatrix} \begin{bmatrix} v_1 \\ v_2 \end{bmatrix} \tag{49}$$

The reduced-order dynamic compensator was designed as follows. To achieve the dynamics of Eq. (49), $\boldsymbol{P}'(s)$ was defined as

$$\boldsymbol{P}'(s) = \begin{bmatrix} (s+1) & 0 \\ 0 & (s+1) \end{bmatrix} \boldsymbol{P}(s) \tag{50}$$

Using Eqs. (37) and (50) leads to the definitions of $\boldsymbol{F}$ and $\boldsymbol{E}$,

$$\boldsymbol{F} = \boldsymbol{C} + \boldsymbol{CA} \tag{51a}$$

$$\boldsymbol{E} = \boldsymbol{CB} \tag{51b}$$

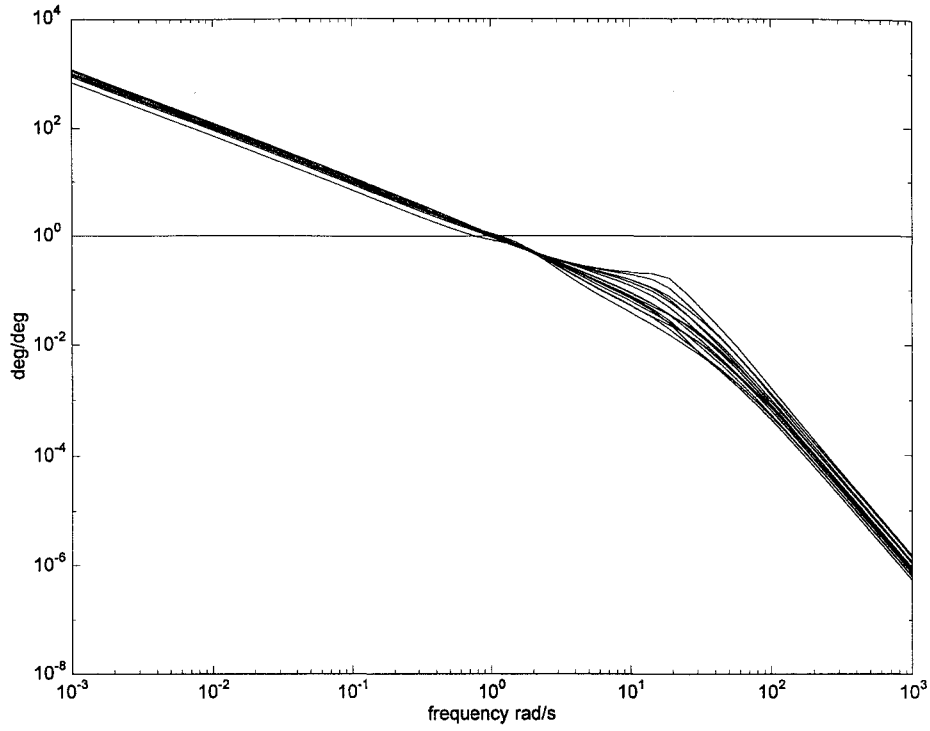

Fig. 2 Magnitude β/v_1 with yaw-rate loop.

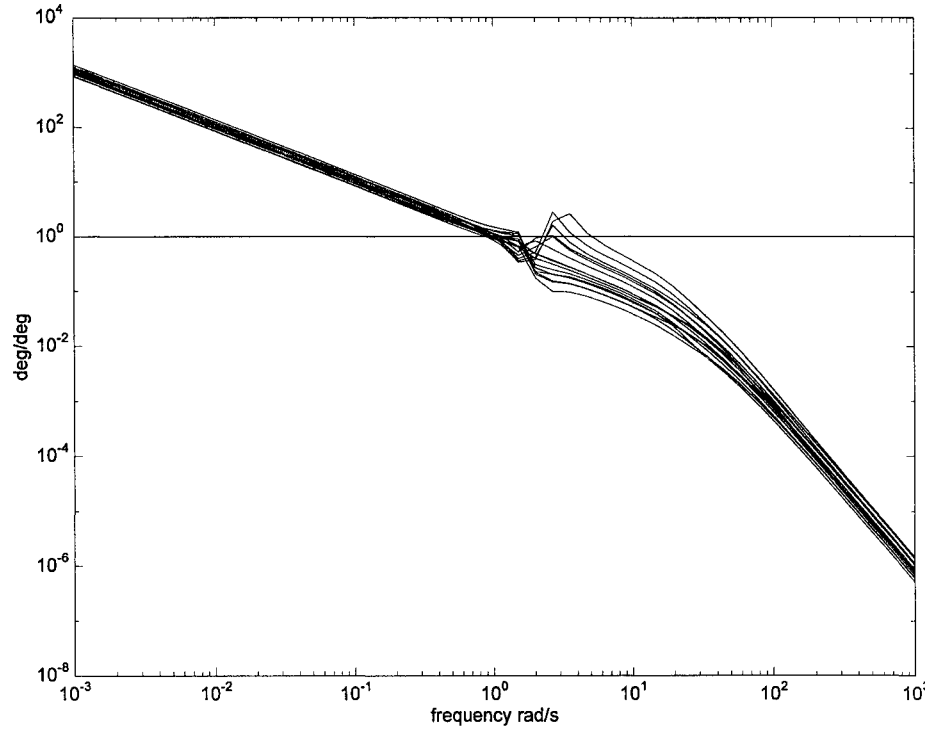

Fig. 3 Magnitude β/v_1 without yaw-rate loop.

where $\boldsymbol{E}$ is right invertible so that a right inverse of $\boldsymbol{P}'(s)$ may be found. This is given using the modified formulation of Eq. (38) as

$$\dot{\boldsymbol{x}}_G = \left(\boldsymbol{A} - \boldsymbol{B}\boldsymbol{E}_R^{-1}\boldsymbol{F}\right)\boldsymbol{x}_G + \boldsymbol{B}\boldsymbol{E}_R^{-1}\boldsymbol{v} + \boldsymbol{H}_{\text{obs}}(\boldsymbol{x} - \boldsymbol{x}_G) \quad (52a)$$

$$\boldsymbol{u} = \boldsymbol{E}_R^{-1}(\boldsymbol{v} - \boldsymbol{F}\boldsymbol{x}_G) \quad (52b)$$

This compensator yields the desired dynamics of Eq. (49). $\boldsymbol{H}_{\text{obs}}$ was selected to be the diagonal matrix

$$\boldsymbol{H}_{\text{obs}} = \begin{bmatrix} 1 & 0 & 0 \\ 0 & 1 & 0 \\ 0 & 0 & 5 \end{bmatrix} \quad (53)$$

This puts a low gain on the errors in $x_1 = \beta$ and $x_2 = p$ but puts a higher gain on the error in $x_3 = r$, causing the r loop to crossover at about 5 rad/s. This term increases the Dutch-roll damping by moving the poles from the eigenvalues of $\boldsymbol{A}$ to those of $(\boldsymbol{A} - \boldsymbol{H}_{\text{obs}})$, as noted in Eq. (41). The choice of $\boldsymbol{H}_{\text{obs}}$ can be made arbitrarily without adversely affecting the good decoupling properties of $\boldsymbol{G}(s)$. The remaining poles are located at the eigenvalues of $(\boldsymbol{A} - \boldsymbol{B}\boldsymbol{E}_R^{-1}\boldsymbol{F})$, which are the transmission zeros of $\boldsymbol{P}'(s)$. For the nominal flight condition the transmission zeros are located at -60.139 and two at -1. The two zeros at $s = -1$ were introduced through the definition of $\boldsymbol{P}'(s)$ in Eq. (50), whereas the large zero comes from $\boldsymbol{P}(s)$.

Despite having only three states, $\boldsymbol{G}(s)$ works well at decoupling p and β. It is robust to realistic uncertainties in the $\boldsymbol{B}$ matrix, and the

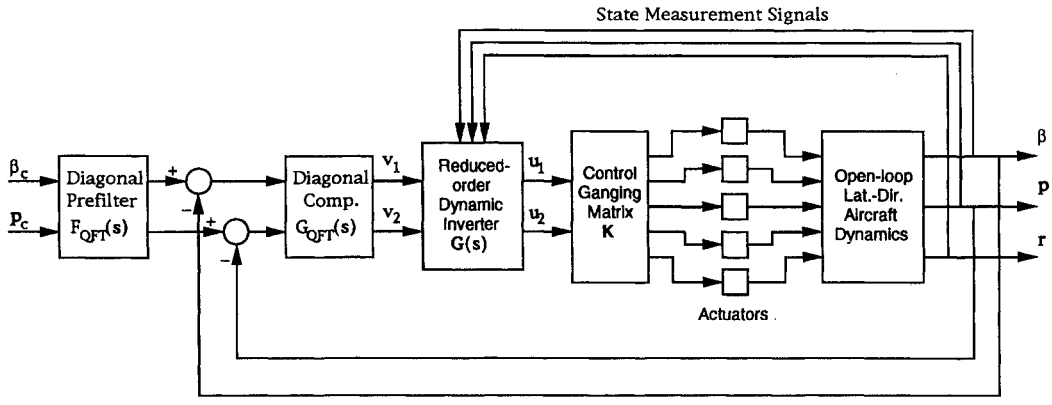

Fig. 4 Improved control structure.

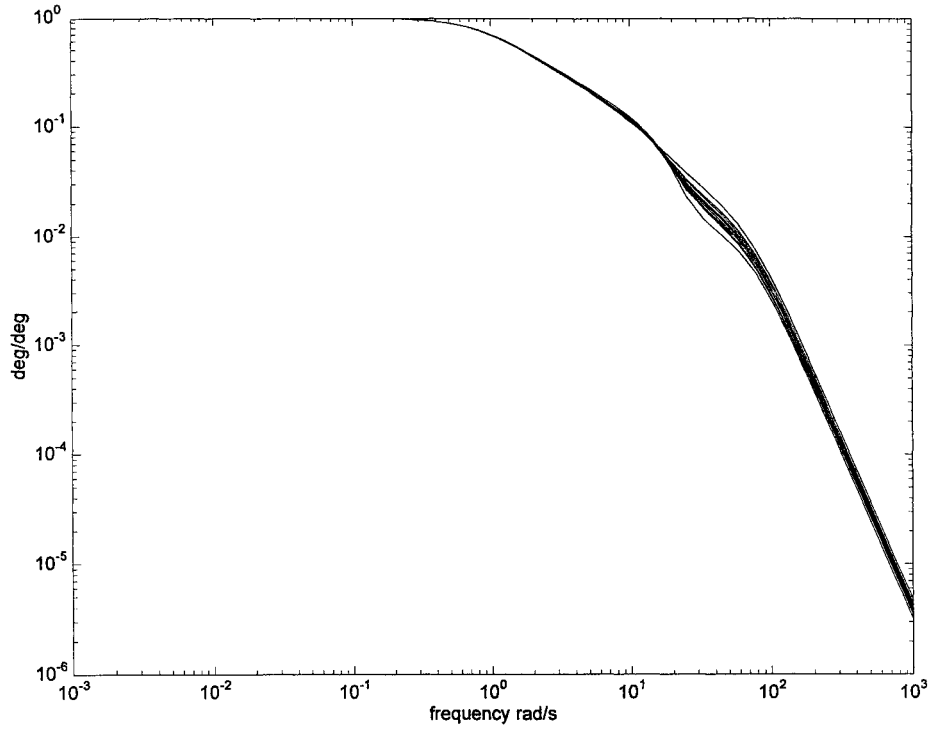

Fig. 5 Magnitude of β/v_1 for three-state $G(s)$.

internal modes are well damped. Bode magnitude plots of $\boldsymbol{P}(s)\boldsymbol{G}(s)$ for all 15 flight conditions with actuators included are shown in Fig. 5. Because $\boldsymbol{G}(s)$ is scheduled with flight condition, all of the flight conditions have a similar level of decoupling [compare with Fig. 2, where $\boldsymbol{G}(s)$ was not scheduled].

As stated earlier a static feedback was also designed for this model. This assumes that the states p, r, and β are readily available measurements. The control law uses the same $\boldsymbol{E}$ and $\boldsymbol{F}$ matrices as before, Eqs. (51a) and (51b). The input to the plant $\boldsymbol{u}$ is given by Eq. (52b) with $\boldsymbol{x}_G$ replaced by the state measurements $\boldsymbol{x}$:

$$\begin{aligned}\boldsymbol{u} &= \boldsymbol{E}_R^{-1}(\boldsymbol{v} - \boldsymbol{F}\boldsymbol{x}) \\ &= -(\boldsymbol{C}\boldsymbol{B})^{-1}(\boldsymbol{C} + \boldsymbol{C}\boldsymbol{A})\boldsymbol{x} + (\boldsymbol{C}\boldsymbol{B})^{-1}\boldsymbol{v} \qquad (54)\end{aligned}$$

This control law has no dynamics because it involves only static state feedback. It should give the desired dynamics of Eq. (49). The controller was readily implemented, but, surprisingly, when coupled to the full-order model, which includes the actuator dynamics, it produced a terribly unstable system with a pole far into the right-half plane at $s = 60$. Such an unstable system cannot be stabilized using the outer loops, which have bandwidth below 10 rad/s.

The instability can be explained by examining the return ratios with the loops opened at the control actuators. Figure 6 shows Bode plots of these return ratios for the nominal flight condition. Two of the return ratios, u_1/u_1 and u_1/u_2 (solid lines), have a crossovers in excess of 60 rad/s. This is because the dynamic inversion attempts to place the pole of its zero dynamics at the zero of $\boldsymbol{P}(s)$, which is located at -60.139 rad/s. This leads to one or more of the state feedback loops (probably yaw rate) having very high bandwidth. The phase lag introduced by the actuators at 60 rad/s was not taken into account in the design of the state feedback loops. The unmodeled phase lag is sufficient to destabilize this fast mode. Interestingly, this problem does not occur when $\boldsymbol{G}(s)$ given by Eq. (52) was used. The dynamic $\boldsymbol{G}(s)$ still introduces a pole at -60.139 rad/s, but this pole is completely internal to $\boldsymbol{G}(s)$ itself, and its location is not dependent on transmission through the actuators. It is, in general, quite reasonable to neglect the actuator dynamics at frequencies below 10 rad/s, where the rigid-body modes of the aircraft lie, and this is why it was so surprising that the static feedback failed so badly. This experience should serve as a warning to designers to check the zero dynamics before applying dynamic inversion. This problem could have been avoided by choosing an alternative to β as an output. A good choice might be $\beta - 0.2r$, which gives a transmission zeros at $s = -4.726$.

Plants with Right-Half Plane Zeros

Systems with right-half plane (RHP) transmission zeros pose the biggest problems because the zeros cannot be moved using state feedback before computing the inverse. Usually, the preferred and simplest means of handling systems with RHP zeros is to redefine the

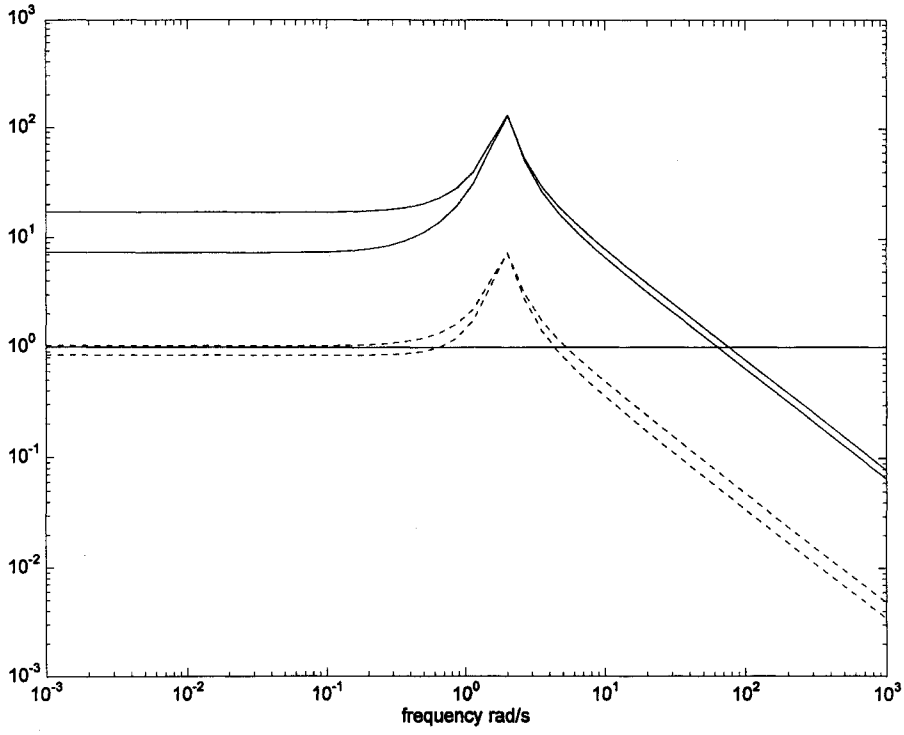

Fig. 6 Magnitude of u_j vs u_i, where $i, j = \{1, 2\}$ for static feedback.

outputs as some combination of the current outputs and other states that yield composite signals with left-half plane zeros. If this is not acceptable, then it is necessary to ensure that any RHP zeros of $\boldsymbol{P}(s)$ are also zeros of $\boldsymbol{P}(s)\boldsymbol{G}(s)$. The RHP zeros cannot be canceled by poles in $\boldsymbol{G}(s)$. Because of the need to factor out polynomial terms, a neat state-space form for $\boldsymbol{G}(s)$ was not found, instead matrix transfer functions were used.

Example 3: Decoupling Roll and Lateral Acceleration

As an example, consider the cancellation control law described in Ref. 9. The aircraft model has a small unstable pole corresponding to the spiral mode. The outputs that are to be decoupled are p_s and ny_{cg}, which are stability axis roll rate and lateral acceleration at the mass center, respectively, and ny_{cg} is nonminimum phase with respect to control inputs and so yields a challenging inversion design. An initial decoupling step yields the transfer function matrix relating pseudoinputs u_1 and u_2 to outputs p_s and ny_{cg}:

$$\begin{bmatrix} p_s \\ ny_{cg} \end{bmatrix} = \boldsymbol{P}(s) \begin{bmatrix} u_1 \\ u_2 \end{bmatrix} = \begin{bmatrix} 10/(s+10) & 0 \\ P_{21}(s) & P_{22}(s) \end{bmatrix} \begin{bmatrix} u_1 \\ u_2 \end{bmatrix} \tag{55}$$

where

$$P_{21}(s) = \frac{-0.33(s^2 - 0.814s + 1.85^2)(s + 4.22)}{(s - 0.072)(s + 0.55)(s + 10)} \tag{56a}$$

$$P_{22}(s) = \frac{-1.038(s + 0.0011)(s - 6.29)(s + 7.54)}{(s - 0.072)(s + 0.55)(s + 10)} \tag{56b}$$

This system can be diagonalized by forming a regulated variable, $ny_{rv} = ny_{cg} + K_r r_s$. The constant gain K_r is chosen so that the resulting transfer function matrix with inputs u_1 and u_2 and outputs p_s and ny_{rv} will no longer have a RHP zero. The problem then is that the decoupling controller will decouple P_s and ny_{rv} but not p_s and ny_{cg}. If this is unacceptable, then it is necessary to design a decoupling controller without canceling the RHP zero. The procedure starts by closing an inner loop from ny_{cg} to u_2 via a feedback compensator $H(s)$ to stabilize the spiral mode:

$$H(s) = \frac{(s + 0.55)(s + 10)}{1.038(s + 0.01)(s + 6.29)(s + 7.54)} \tag{57}$$

This stabilizes the spiral mode and gives

$$\begin{bmatrix} p_s \\ ny_{cg} \end{bmatrix} = \boldsymbol{P}_e(s) \begin{bmatrix} u_1 \\ v_2 \end{bmatrix} = \begin{bmatrix} 10/(s+10) & 0 \\ P_{e_{21}}(s) & P_{e_{22}}(s) \end{bmatrix} \begin{bmatrix} u_1 \\ v_2 \end{bmatrix} \tag{58a}$$

where

$$P_{e_{21}}(s) = \frac{-0.33(s^2 - 0.814s + 1.85^2)(s + 4.22)(s + 0.01)(s + 6.29)}{(s + 0.55)(s + 10)(s + 0.004)(s + 1.65)(s + 3.58)} \tag{58b}$$

$$P_{e_{22}}(s) = \frac{-1.038(s + 0.0011)(s - 6.29)(s + 7.54)(s + 0.01)(s + 6.29)}{(s + 0.55)(s + 10)(s + 0.004)(s + 1.65)(s + 3.58)} \tag{58c}$$

A decoupling controller $\boldsymbol{G}(s)$ is designed by computing the matrix inverse of $\boldsymbol{P}_e(s)$. The factor $(s - 6.29)$ in the denominator of the inverse is eliminated by multiplying the whole matrix by the all-pass, $(6.29 - s)/(s + 6.29)$. Poles were added (at $s = -10$ and -2) to make $\boldsymbol{G}(s)$ proper. The resulting decoupling control is

$$\begin{bmatrix} u_1' \\ u_2' \end{bmatrix} = \boldsymbol{G}(s) \begin{bmatrix} v_1 \\ v_2 \end{bmatrix} = \begin{bmatrix} G_{11}(s) & 0 \\ G_{21}(s) & G_{22}(s) \end{bmatrix} \begin{bmatrix} v_1 \\ v_2 \end{bmatrix} \tag{59}$$

where

$$G_{11}(s) = \frac{(6.29 - s)}{(s + 6.29)} \frac{10}{(s + 10)} \frac{1}{P_{e_{11}}(s)} = \frac{(6.29 - s)}{(s + 6.29)} \tag{60a}$$

$$G_{21}(s) = \frac{(6.29 - s)}{(s + 6.29)} \frac{10}{(s + 10)} \frac{\left(-P_{e_{21}}(s)\right)}{P_{e_{11}}(s) P_{e_{22}}(s)}$$

$$= \frac{0.33(s^2 - 0.814s + 1.85^2)(s + 4.22)}{1.038(s + 0.0011)(s + 6.29)(s + 7.54)} \tag{60b}$$

$$G_{22}(s) = \frac{(6.29 - s)}{(s + 6.29)} \frac{2}{(s + 2)} \frac{1}{P_{e_{22}}(s)}$$

$$= \frac{2(s + 0.55)(s + 10)(s + 0.004)(s + 1.65)(s + 3.58)}{1.038(s + 0.0011)(s + 0.1)(s + 2)(s + 6.29)^2(s + 7.54)} \tag{60c}$$

which yields the overall dynamics $\boldsymbol{P}_e(s)\boldsymbol{G}(s)$ giving

$$\begin{bmatrix} p_s \\ ny_{cg} \end{bmatrix} = \begin{bmatrix} \dfrac{(6.29-s)}{(s+6.29)}\dfrac{10}{(s+10)} & 0 \\ 0 & \dfrac{(6.29-s)}{(s+6.29)}\dfrac{2}{(s+2)} \end{bmatrix} \begin{bmatrix} r_1 \\ r_2 \end{bmatrix} \tag{61}$$

Notice that the zero at $s = 6.29$ appears in both channels and is the unavoidable cost paid for exact decoupling of p_s from the nonminimum phase output ny_{cg}.

Conclusions

A method of designing exact decoupling control laws for multivariable systems was presented. This permits a plant to be diagonalized, making it much easier to design outer feedback loops for the multivariable system using SISO-based techniques such as conventional loop-shaping and QFT. Certain basic requirements must be met to permit decoupling, but these are not overly restrictive. The case where the plant dynamics are stable and minimum phase can be found readily using a purely state-space approach. When the plant dynamics have unstable poles, additional feedback loops must be used to provide internal stability. When the plant has RHP transmission zeros a direct, state-space approach is not readily apparent, and the solution is necessarily more complicated.

Appendix: Transmission Zeros of $[A, B, F, E]$

Proposition: The zeros of the system $[\boldsymbol{A}, \boldsymbol{B}, \boldsymbol{C}, \boldsymbol{D}]$ are also transmission zeros of the system $[\boldsymbol{A}, \boldsymbol{B}, \boldsymbol{F}, \boldsymbol{E}]$, where $\boldsymbol{E}$ and $\boldsymbol{F}$ are defined by Eq. (16).

The transmission zeros of $[\boldsymbol{A}, \boldsymbol{B}, \boldsymbol{C}, \boldsymbol{D}]$ are given by finding a scalar ζ_P and two nonzero vectors $\boldsymbol{z}_P$ and $\boldsymbol{w}_P$, such that

$$\begin{bmatrix} (\zeta_P \boldsymbol{I} - \boldsymbol{A}) & -\boldsymbol{B} \\ \boldsymbol{C} & \boldsymbol{D} \end{bmatrix} \begin{bmatrix} \boldsymbol{z}_P \\ \boldsymbol{w}_P \end{bmatrix} = \begin{bmatrix} \boldsymbol{0} \\ \boldsymbol{0} \end{bmatrix} \tag{A1}$$

We wish to prove that the same scalar ζ_P and two nonzero vectors $\boldsymbol{z}_P$ and $\boldsymbol{w}_P$ satisfy

$$\begin{bmatrix} (\zeta_P \boldsymbol{I} - \boldsymbol{A}) & -\boldsymbol{B} \\ \boldsymbol{F} & \boldsymbol{E} \end{bmatrix} \begin{bmatrix} \boldsymbol{z}_P \\ \boldsymbol{w}_P \end{bmatrix} = \begin{bmatrix} \boldsymbol{0} \\ \boldsymbol{0} \end{bmatrix} \tag{A2}$$

Proof: Clearly the first block row of Eq. (A2) is satisfied because it is identical to that of Eq. (A1). Examining the block rows of Eq. (A1) individually we have

$$(\zeta_P \boldsymbol{I} - \boldsymbol{A})\boldsymbol{z}_P - \boldsymbol{B}\boldsymbol{w}_P = \boldsymbol{0} \tag{A3a}$$

$$\boldsymbol{C}\boldsymbol{z}_P + \boldsymbol{D}\boldsymbol{w}_P = \boldsymbol{0} \tag{A3b}$$

We need to prove that

$$\boldsymbol{F}\boldsymbol{z}_P + \boldsymbol{E}\boldsymbol{w}_P = \boldsymbol{0} \tag{A4}$$

Now examine the individual rows of Eq. (A3b):

$$\boldsymbol{C}_i\boldsymbol{z}_P + \boldsymbol{D}_i\boldsymbol{w}_P = \boldsymbol{0} \tag{A5}$$

If $d_i = 0$, then $\boldsymbol{D}_i$ is nonzero, and we have from definitions (16a) and (16b) that $\boldsymbol{D}_i = \boldsymbol{E}_i$ and $\boldsymbol{C}_i = \boldsymbol{F}_i$ so that the ith row of Eq. (A4) is trivially satisfied.

In the case $d_i = 1$, then $\boldsymbol{D}_i$ is zero, and so Eq. (A5) yields $\boldsymbol{C}_i\boldsymbol{z}_P = 0$. Premultiplying Eq. (A3a) by $\boldsymbol{C}_i$ gives

$$\zeta_P \boldsymbol{C}_i\boldsymbol{z}_P - \boldsymbol{C}_i\boldsymbol{A}\boldsymbol{z}_P - \boldsymbol{C}_i\boldsymbol{B}\boldsymbol{w}_P = \boldsymbol{0} \tag{A6}$$

The first term in Eq. (A6) is zero. Furthermore, if $d_i = 1$, then we have from definitions (16a) and (16b) that $\boldsymbol{F}_i = \boldsymbol{C}_i\boldsymbol{A}$ and $\boldsymbol{E}_i = \boldsymbol{C}_i\boldsymbol{B}$ so that Eq. (A6) satisfies the ith row of Eq. (A4): $\boldsymbol{F}_i\boldsymbol{z}_P + \boldsymbol{E}_i\boldsymbol{w}_P = \boldsymbol{0}$.

Suppose $d_i \geq 2$, then $\boldsymbol{D}_i = \boldsymbol{0}$. Furthermore, $\boldsymbol{C}_i\boldsymbol{A}^j\boldsymbol{B} = \boldsymbol{0}$ for all integers, $0 \leq j < (d_i - 1)$.

Lemma: For $0 \leq j < (d_i - 1)$ we have $\boldsymbol{C}_i\boldsymbol{A}^{(j+1)}\boldsymbol{z}_P = \boldsymbol{0}$.

Proof of lemma: Premultiplying Eq. (A3a) by $\boldsymbol{C}_i\boldsymbol{A}^j$ yields

$$\zeta_P \boldsymbol{C}_i\boldsymbol{A}^j\boldsymbol{z}_P - \boldsymbol{C}_i\boldsymbol{A}^{(j+1)}\boldsymbol{z}_P - \boldsymbol{C}_i\boldsymbol{A}^j\boldsymbol{B}\boldsymbol{w}_P = \boldsymbol{0} \tag{A7}$$

The third term is zero in the specified range of j. If we can show that the first term is zero, then we have $\boldsymbol{C}_i\boldsymbol{A}^{(j+1)}\boldsymbol{z}_P = \boldsymbol{0}$. Proceeding inductively, let $j = 0$, then Eq. (A7) yields

$$\zeta_P \boldsymbol{C}_i\boldsymbol{z}_P - \boldsymbol{C}_i\boldsymbol{A}\boldsymbol{z}_P - \boldsymbol{C}_i\boldsymbol{B}\boldsymbol{w}_P = \boldsymbol{0} \tag{A8}$$

The first term in Eq. (A8) is zero from Eq. (A4); the last term is zero by definition of d_i and so this implies $\boldsymbol{C}_i\boldsymbol{A}\boldsymbol{z}_P = \boldsymbol{0}$. Using this result and setting $j = 1$ in Eq. (A7) completes the proof of the lemma.

Continue with the case that $d_i \geq 2$. Premultiplying Eq. (A3a) by $\boldsymbol{C}_i\boldsymbol{A}^{(d_i-1)}$ yields

$$\zeta_P \boldsymbol{C}_i\boldsymbol{A}^{(d_i-1)}\boldsymbol{z}_P - \boldsymbol{C}_i\boldsymbol{A}^{d_i}\boldsymbol{z}_P - \boldsymbol{C}_i\boldsymbol{A}^{(d_i-1)}\boldsymbol{B}\boldsymbol{w}_P = \boldsymbol{0} \tag{A9}$$

From the lemma, the first term is zero. Using the definitions in Eqs. (16a) and (16b), Eq. (A9) is recognized to be $\boldsymbol{F}_i\boldsymbol{z}_P + \boldsymbol{E}_i\boldsymbol{w}_P = \boldsymbol{0}$.

Thus, we have shown that for all possible values of d_i, Eqs. (A3a) and (A3b) imply

$$\boldsymbol{F}_i\boldsymbol{z}_P + \boldsymbol{E}_i\boldsymbol{w}_P = \boldsymbol{0}$$

This completes the proof of the Proposition.

References

[1]Horowitz, I. M., *Quantitative Feedback Design Theory (QFT)* Vol. 1, QFT Publications, Boulder, CO, 1993, Chap. 14.

[2]Snell, A., and Hess, R. A., "Robust Decoupled Flight Control Design with Actuator Saturation," *Journal of Guidance, Control, and Dynamics*, Vol. 21, No. 3, 1998, pp. 361–367; also AIAA Paper 97-3778, 1997.

[3]Enns, D., Bugajski, D., Hendrick, R., and Stein, G., "Dynamic Inversion: An Evolving Methodology for Flight Control Design," *International Journal of Control*, Vol. 59, No. 1, 1994, pp. 71–91.

[4]Lane, S., and Stengel, R. F., "Flight Control Design Using Nonlinear Inverse Dynamics," *Automatica*, Vol. 24, No. 4, 1988, pp. 471–483.

[5]Singh, S. N., and Rugh, W. J., "Decoupling in a Class of Nonlinear Systems by State Variable Feedback," *Journal of Dynamic Systems, Measurement and Control*, Vol. 94, Dec. 1972, pp. 323–329.

[6]Menon, P. K. A., Badgett, M. E., Walker, R. A., and Duke, E. L., "Nonlinear Flight Test Trajectory Controls for Aircraft," *Journal of Guidance, Control, and Dynamics*, Vol. 10, No. 1, 1987, pp. 67–72.

[7]Snell, S. A., Enns, D. F., and Garrard, W. L., "Nonlinear Inversion Flight Control for a Supermaneuverable Aircraft," *Journal of Guidance, Control, and Dynamics*, Vol. 15, No. 3, 1992, pp. 976–984.

[8]Slotine, J. J., and Li, W., *Applied Nonlinear Control*, Prentice-Hall, Englewood Cliffs, NJ, 1991, Chap. 6.

[9]Snell, S. A., "Cancellation Control Law for Lateral-Directional Dynamics of a Supermaneuverable Aircraft," AIAA Paper 93-3775, Aug. 1993.